

Fault diagnostic system based on approximate reasoning

Pavle Boškosi¹, Bojan Musizza¹, Janko Petrovčič¹, and Đani Juričić¹

¹ *Institute Jožef Stefan, Ljubljana, Slovenia*
(pavle.boskoski|bojan.misuzza|janko.petrovic|dani.juricic)@ijs.si

ABSTRACT

Guaranteeing 100% fault free products is becoming an emerging standard in many branches of manufacturing. This paper addresses the design of an end-quality diagnostic system for detection of mechanical faults in electronically commutated motors. One of the main requirements of an end-quality diagnostic system is its ability for detecting faults in their earliest stages. Main issue in detecting final products with such faults lies in the fact that the faulty product is indistinguishable from the fault-free one. In order to overcome this problem, we have performed the feature extraction method using the spectral kurtosis method. These features were used as an input to the fault localization module, which is based on approximate reasoning technique known as Transferable Belief Model (TBM). Results show that the diagnostic system comprising spectral kurtosis and transferable belief model successfully isolates the most common mechanical faults. Additionally the strength of conflict can be used as a measure of certainty of the diagnostic results. The performance of the diagnostic system was evaluated on a batch of 60 motors.

1 INTRODUCTION

Designing an efficient fault diagnosis system has always been a challenging task. The goal of 100% fault-free end-products is becoming an industry standard. In this paper we focus on designing a diagnostic system for quality assurance in manufacturing of electronically commutated (EC) motors.

In the research domain there is an impressive body of literature that addresses the issues of rotational machines. Xu and Marangoni did extensive research in the area of shaft misalignment and imbal-

ance faults, and concluded that these faults were directly connected with the shaft rotating speeds (Xu and Marangoni, 1994a; 1994b). McFadden and Smith laid the basic principles of the bearing fault detection (McFadden and Smith, 1984) and afterwards (Tandon and Choudhury, 1999) devised a model for bearing faults defining the characteristic frequencies that are produced by a particular localized fault.

Extensive work has also been done in the area of signal processing methods. Time-frequency wavelet analysis of the electrical current was used by (Kar and Mohanty, 2006) and (Zarei and Poshtan, 2007) for fault detection in electrical motors. (Sawalhi *et al.*, 2007) used spectral kurtosis for bearing fault detection. (Rubini and Meneghetti, 2001) and (Ho and Randall, 2000) used envelope analysis for fault detection in rotational machinery. Additionally cyclostationary analysis of the vibration signals have been applied with satisfactory results (Randall *et al.*, 2001; Antoni, 2007).

The problem of fault detection in electrical motors has also been addressed by many authors, however most of their work concentrates on fault detection in AC electrical motors, like (Röpke and Filbert, 1994; Sasi *et al.*, 2001; Didier *et al.*, 2007). Unlike the conventional AC motors, fault detection for brushless DC motor has been addressed by fewer authors e.g. (Juričić *et al.*, 2001).

Apart from the abundance of fault detection algorithms and signal processing techniques, very few published works address the design of industrial operating prototypes of diagnostic systems. One such system designed for vacuum cleaner motors based on vibration and sound analysis was done by (Benko *et al.*, 2005) and (Tinta *et al.*, 2005).

The tasks of any diagnostic procedure can be subdivided into fault detection by analytic and heuristic symptom generation and fault diagnosis (Isermann, 2000). The process of symptom generation should be able to produce distinctive features for each particular fault. Based on these extracted feature an autonomous fault diagnostic has to be able to determine whether the observed motor is fault-free or not. Furthermore, in cases of positive fault detection the diagnostic mod-

This is an open-access article distributed under the terms of the Creative Commons Attribution 3.0 United States License, which permits unrestricted use, distribution, and reproduction in any medium, provided the original author and source are credited.

ule should be able to isolate the source of the fault.

Envelope analysis method has been one of the most common approaches used for symptom generation. This method has proven to be sufficient for detection of severe faults. However, in cases where the vibrations produced by an incipient fault are masked by surrounding vibration sources or additive noise, a simple envelope analysis becomes inefficient. Such were the cases of EC motors with improper bearing lubrication or bearing damages due to inappropriate mounting. The main problem in these cases is that the extracted features resemble the fault-free case, so the faulty EC motor under investigation becomes indistinguishable from the fault-free ones. Several authors have shown that a significant increase in analysis sensitivity can be obtained by calculating the envelope spectrum of the acquired vibration signal filtered within specially selected frequency band (Staszewski, 1998; Wang, 2001). In our case, the acquired vibration signals were analyzed by spectral kurtosis (SK) method (Antoni, 2006; Sawalhi *et al.*, 2007). The spectral kurtosis method is an effective tool for determining the frequency bands in which the examined signal exhibits high amount of impulsiveness. Thus by filtering the signal in the proposed frequency bands the fault impulses become more distinguishable. The spectral analysis of the filtered signals in the selected frequency bands have shown significant increase in sensitivity, allowing unambiguous detection of all faults, thus completing the symptom generation task.

The next step in the process of end-quality assessment was the fault diagnosis procedure. The fault diagnosis procedure may be considered as a task of matching the observed feature patterns with a pre-determined set of patterns representing particular mechanical faults (Jardine *et al.*, 2006). Although, some machine learning methods have been used for this purpose, for fault diagnosis of EC motors we have selected an approximate reasoning technique called transferable belief model (TBM). The TBM method was selected due to the possibilities of incorporating expert's knowledge as well as its adaptability towards unforeseen errors. The main idea was to combine an efficient signal processing method with an accurate diagnostic algorithm, thus obtaining accurate final quality assessment system.

The paper is organized in the following manner. The characteristics of EC motors and an overview of the assessment rig are given in Sections 2 and 3. Feature extraction and the theory behind the applied signal processing technique are presented in Section 4. Results of the application of the feature extraction process are given in Section 5. Brief overview of the theory behind the Transferable Belief Model is presented in Section 6. The implementation of the TBM and the results of the validation of the diagnostic system are given in the Section 7.

2 ELECTRONICALLY COMMUTATED MOTORS

In a conventional DC motor, brushes make mechanical contact with a set of electrical contacts on the rotor's commutator, forming an electrical circuit between the DC electrical source and the armature windings. In

a electronically commutated (EC) motors, the permanent magnets rotate and the armature remains static. Since the armature is static the commutator becomes obsolete. In order to generate a rotating magnetic field, the brush-system/commutator assembly is replaced by an electronic controller.

3 THE ASSESSMENT RIG

The prototype of the assessment rig is shown in Figure 1. The motor under investigation is positioned vertically. It is suspended on rubber dampers, which are fixed to a pedestal. The motor runs without any load during all experimental runs and under a constant speed $f_{rot} = 38\text{Hz}$.

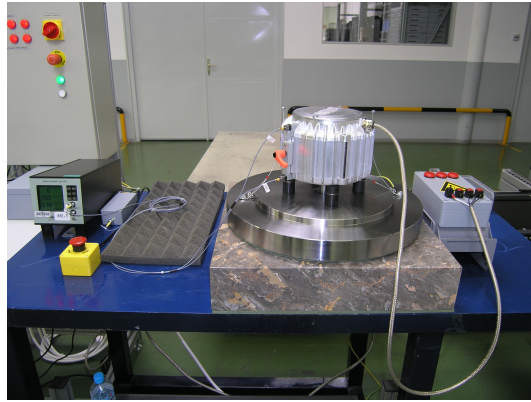


Figure 1: The prototype assessment point

Motor vibrations were measured on the motor housing. The signal was conditioned by a low-pass filter with the cut-off frequency at 22kHz and then sampled at 60kHz. The following faults were investigated:

- bearing inner race fault,
- bearing outer race fault,
- bearing roller element fault,
- lack of lubricant in the bearing and
- rotor unbalance.

Due to lack of historical vibration measurements covering the listed mechanical faults we have prepared a set of artificially damaged bearings. The damages were artificially introduced using electric erosion procedure, by eroding small areas either on the bearing inner, outer or roller element surface. Besides this mechanical faults, the lack of lubrication fault was done by cleaning several bearings with *tetrachloroethylene*, thus removing all present grease in the bearing. The unbalance fault was tested in two ways: (i) adding different weights in the shaft key and (ii) by installing unbalanced rotor. With such configuration of artificial faults, we have obtained a set of most probable mechanical faults with different stages of fault severity.

Both motor bearings are FAG 6205. The bearing's characteristic defect frequencies are shown in Table 1 (Tandon and Choudhury, 1999).

The frequencies given in Table 1 are calculated for a bearing with a stationary outer race using the expressions shown in Eq. (1).

Table 1: Calculated bearing frequencies for FAG 6205

Bearing fault	f/f_{rot}
Ball pass frequency inner (BPFI)	5.415
Ball pass frequency outer (BPFO)	3.585
Fundamental train frequency (FTF)	0.398
Ball spin frequency (BSF)	2.375

$$\begin{aligned}
BPFO &= \frac{Zf_{rot}}{2} \left(1 - \frac{d}{D} \cos\alpha\right) \\
BPFI &= \frac{Zf_{rot}}{2} \left(1 + \frac{d}{D} \cos\alpha\right) \\
FTF &= \frac{f_{rot}}{2} \left(1 - \frac{d}{D} \cos\alpha\right) \\
BSF &= \frac{Df_{rot}}{2d} \left(1 - \left(\frac{d}{D} \cos\alpha\right)^2\right),
\end{aligned} \tag{1}$$

where Z is the number of rolling elements, d is the rolling element diameter, D is the pitch diameter, α is the contact angle and f_{rot} is the inner ring rotational speed.

4 FEATURE EXTRACTION TECHNIQUES

Rotor unbalance and misalignment faults

The vibration signature produced by the presence of these faults is rather simple. According to (Xu and Marangoni, 1994a; 1994b) rotor unbalance and misalignment faults produce vibrations that have strong spectral components at rotational speed f_{rot} and its higher harmonics, usually $2 \times f_{rot}$ and $4 \times f_{rot}$. An increase in any of these three listed harmonics can be attributed to the presence of rotor unbalance.

Bearing faults

Most frequently, bearing faults include surface damage of the inner or outer rings as well as the rolling bearing elements. When such a fault appears, the passing rolling element will generate an impact which will excite damped oscillations defined by the modes of the bearing and its support. Due to the rotation, the vibration produced by a faulty bearing will consist of similar periodic bursts dominated by the resonance frequency of the structure. Since there are random speed fluctuations as well as some random slip, these impulses almost never repeat in truly periodic manner. That is why a simple statistical model of bearing vibration defined by (Randall *et al.*, 2001), was used for further analysis

$$x(t) = \sum_i A_i s(t - iT - \tau_i) + n(t), \tag{2}$$

where $x(t)$ is the vibration signal, A_i is the randomly changing impact amplitude, $s(t)$ is system impulse response, T is the average time between each impact, and τ_i is the time lag of the i^{th} impact due to the random slip.

4.1 Spectral Kurtosis

According to the Eq. (2), bearing faults are characterized by quasi-periodic impulses. Thus, for the purpose of fault detection, the most suitable frequency band would be the one where these impulses are most clearly visible. One possibility is to use the method called spectral kurtosis.

The spectral kurtosis (SK) method was firstly introduced by (Dwyer, 1983), as a method that is able to distinguish between transients (impulses and unsteady harmonic components) and stationary sinusoidal signals in background Gaussian noise.

Spectral kurtosis takes high values for frequency bands where the vibration signal $x(t)$ defined with Eq.(2) is dominated by the corresponding impulses, and it takes low values for frequency bands where the signal is dominated by the Gaussian noise $n(t)$ or stationary periodic components. If we rewrite the signal from Eq.(2) as

$$x(t) = y(t) + n(t), \tag{3}$$

where

$$y(t) = \sum_i A_i s(t - iT - \tau_i), \tag{4}$$

than the SK values for the signal $x(t)$ contaminated by additive noise $n(t)$ can be calculated as (Antoni and Randall, 2006)

$$K_x(f) = \frac{K_y(f)}{[1 + \rho(f)]^2}, \tag{5}$$

where $K_y(f)$ is the spectral kurtosis of the signal $y(t)$, and $\rho(f)$ is the noise-to-signal ratio for that particular frequency f . The value for $K_y(f)$ can be obtained using the following relation

$$K_y(f) = \frac{S_{4y}(f) - 2S_{2y}^2(f)}{S_{2y}^2(f)}, \tag{6}$$

where $S_{2y}(f)$ and $S_{4y}(f)$ are the second and fourth spectral moments respectively. The maximum of Eq.(5), actually determines the frequency band where the signal-to-noise ratio in the observed signal is the biggest and in the same time the closest to the original, uncontaminated signal, $y(t)$.

The definition of SK given by the Eq.(6) bears resemblance with the statistical definition of kurtosis. However the actual physical interpretation and its ability for detection of non-stationary transients in signals is not so obvious. One way to clarify this issue is to observe the time-frequency characteristic of the vibration signal $x(t)$, defined by Eq. (2). We can consider the changes of the amplitude of particular spectral components of $x(t)$ in time as a stochastic process. The SK method searches for a frequency band where this stochastic process shows highest kurtosis. Such analysis is justified since for non-stationary processes these changes in the amplitudes of some spectral components will be more expressed then in the cases of stationary processes. Consequently, we can use the SK as a indicator for a frequency band where the signal's non-stationarities are most expressed.

5 FAULT SIGNATURES

Since there is no model for the motor or any historical data, the presence of a fault can only be determined by comparing the vibration signal from the examined motor against the vibration signal from a fault-free motor. In order to be able to make a proper comparison all tests were conducted under the same speed ($f_{rot}=38\text{Hz}$), which is the nominal motor speed. The measurements were conducted on a batch of 60 motors, containing different types of faults. The presented fault signatures are taken from a particular experimental runs representing each type of simulated faults.

5.1 Fault-free motor

Under nominal speed f_{rot} , the pulse width modulation has frequency at $f_{pwm} = 5 \times f_{rot}$. The factor 5 originates from the motor construction, i.e. 5 pole brushless DC motor.

The vibration signal of the fault free state is dominated by the three frequencies marked as *PWM*, $10 \times f_{rot} = 387.3\text{Hz}$, and its second harmonic $20 \times f_{rot}$, shown in Figure 2. The first component originates from the pulse with modulation of the power supply f_{pwm} . The other two components at $10 \times f_{rot}$ and $20 \times f_{rot}$ are actually the 2nd and 3rd harmonics of the f_{pwm} .

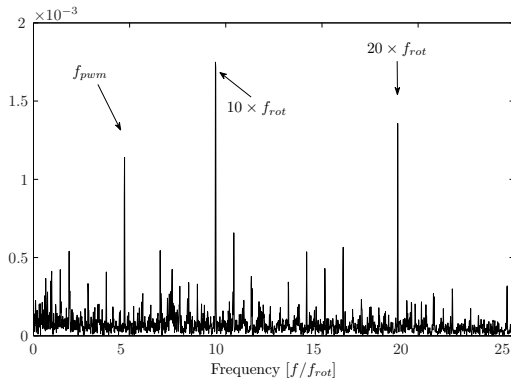


Figure 2: Envelope spectra of the vibration signal from fault-free motor

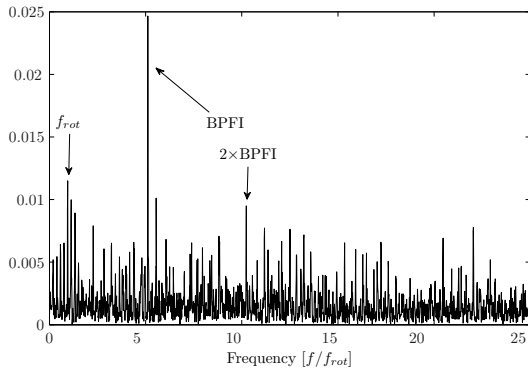


Figure 3: Envelope spectra of the vibration signal for inner race fault

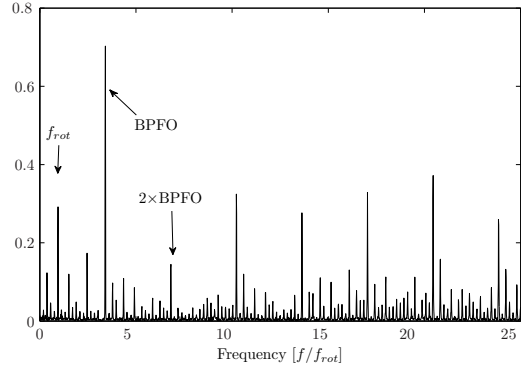


Figure 4: Envelope spectra of the vibration signal for outer race fault

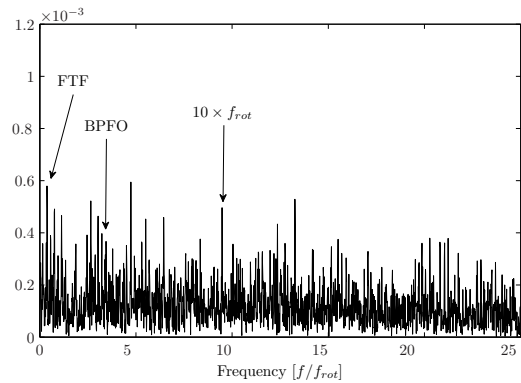


Figure 5: Envelope spectra of the vibration signal for lack of lubrication fault

5.2 Bearing inner and outer race faults

Two separate experiments were done in order to examine the vibration signature in the presence of inner and outer bearing fault respectively.

The envelope spectrum of the vibration signal for the inner race fault is shown in Figure 3. The spectrum is dominated by the BPFI, see (1), and its 2nd harmonic. It should be noticed that the amplitudes of these components are several times larger than the amplitudes of the components in the fault-free case. Similarly, the spectrum of the outer race fault, shown in Figure 4, is dominated by the BPFO and its 2nd harmonic.

Besides the different dominant spectral components, the spectra of bearing inner and outer race faults significantly differ in the amplitude range of the spectral components. The spectral components for the case of outer race fault have significantly larger amplitudes due to the fact that the damage done on the outer race was more severe compared to the damage on the bearing with inner race fault.

5.3 Lack of lubrication

The envelope spectrum for this fault is shown in Figure 5. Unlike the bearing inner and outer race faults this spectrum does not contain any new spectral components compared to the spectrum of the fault-free case. Even more, comparison with the fault-free case

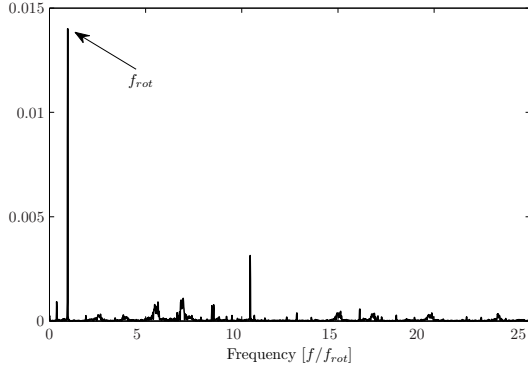


Figure 6: Envelope spectra of the vibration signal for unbalance fault

reveals that the amplitudes of almost all spectral components are smaller. The spectrum is not dominated by the spectral components at $10 \times f_{rot}$ and its second harmonic as it was in the fault-free motor. Similar observation was done by (Singh and Kazzaz, 2009). They noticed that in the case of lack of lubrication the spectrum of the vibration signal has no dominant harmonics. The absence of dominant components as well as lower amplitudes, compared to the fault-free case, makes this fault very difficult to detect.

The spectral component with the largest amplitude is the fundamental train frequency (FTF). This component is not visible in the fault-free state because presence of lubrication damps the vibrations caused by the rolling bearing elements. This effectively removes or significantly attenuates the FTF spectral component. Since there is no lubricant to act as a damper, these vibrations are clearly visible in the envelope spectrum.

Apart from FTF component, the spectrum for lack of lubrication also contains spectral components of bearing outer race fault. This is due to the fact that the BPFO is 9th harmonic of FTF, i.e. $BPFO = Z \times FTF$, where Z is the number of rolling elements. The amplitude of this component is quite smaller than the corresponding one in the case of pure outer ring fault. Since the mentioned components are not present in the fault free case they can be used as an additional feature for detection of this fault.

5.4 Rotor unbalance

This fault is characterized by stronger first and second harmonics of the shaft rotating speed. Accordingly, the fault is most visible in the first harmonic of the rotational speed. The spectrum of the vibration signal for a rotor with unbalance is dominated by the spectral component of the rotational speed f_{rot} (cf. Figure 6). The amplitude is several orders bigger than the one in the fault-free case.

6 FAULT DIAGNOSTICS

Fault diagnostics process consists of fault isolation and identification tasks. The fault isolation task is a process of determination of the kind, location and time of detection of a fault, whereas the fault identification task is a process of determination of the size and time-variant behavior of a fault (Isermann and Ballé,

1997). The task of fault diagnostics of the BLDC motor was done by comparing the features extracted from the acquired vibration signals with a pre-determined set of features for each particular fault obtained from a signal-model, (eg. the bearing principle fault frequency components Eq. (1) in the envelope spectrum). Such approach opens a way for employing several already developed methods for classification or pattern recognition. In this manner, clustering has been one of the most commonly used approaches. Fault diagnosis using clustering method is performed by defining a cluster for each expected fault as well as an additional cluster representing the fault-free products. The determination of the clusters' parameters can be performed using different approaches of supervised or unsupervised learning (Leia *et al.*, 2008). Recently support vector machines (SVM) have been used to optimize the boundary between the adjacent clusters (Jack and Nandi, 2001). Besides clustering approaches, Artificial Neural Networks (ANN) with Genetic Algorithm (GA) optimization have been also used for the purpose of fault diagnosis (Samanta, 2004). Although the results of fault diagnostics using any of these methods are satisfactory, there are several limitations. Firstly, for the purpose of training, the mentioned algorithms require sufficiently high amount of training data. Furthermore, it was not shown how an expert's knowledge or some startard's requirements can be incorporated in the proposed methods. Finally, the training process consisted of only a limited set of faults, and the performance of the methods was not evaluated for the cases of unforeseen faults.

The insufficient amount of training data, and the inability to simulate all possible faults were the main obstacles in using any of the listed machine learning tools for the task of fault diagnosis of EC motors. One way around this limitations is to use some methods from the field of maintenance decision support. In such manner we have selected an approximate reasoning technique called Transferable belief model (TBM). This method allows incorporation of expert's knowledge in the creation of the incidence matrix and also on the selection of features and intervals of their acceptable values. All these information remove the need for high amount of training data, needed in the case of machine learning approaches. Moreover, the cases of unforeseen errors are resolved by using the strength of conflict parameter, which can be treated as measure of uncertainty for the performed diagnosis.

6.1 Transferable belief model

The fault isolation part of the diagnostic system is based on the transferable belief model (TBM) (Smets and Kennes, 1994). Besides the degrees of belief for each fault candidate, the approach also provides a measure for confidence in diagnostic results, referred to as the strength of conflict.

The TBM derives from the Dempster-Shafer theory of evidence by introducing the concept of "open-world". It simply says that the set of all propositions Ω consists of the three subsets: (PP) the set of possible propositions, (IP) impossible propositions and (UP) the unknown propositions. Classical reasoning schemes do not operate with UP.

The purpose of the TBM is to compute the

belief masses for the fault candidates $PP = \{f_1, f_2, \dots, f_n, ff\}$ given the measured features $\{r_1, r_2, \dots, r_M\}$ (Rakar and Juričić, 2002; Juričić *et al.*, 2001). Here ff denotes the fault-free case. There is no need to consider elements of IP , as the beliefs are assigned only to PP . The elements of UP can be transferred to PP if new evidence becomes available. The qualitative relationship between faults and features is expressed in terms of the incidence matrix $\Lambda = [\lambda_{i,j}]$. An entry $\lambda_{i,j} \neq 0$ means that the j^{th} fault triggers the i^{th} feature ($|r_{i,j}| \geq f_i$). The symbol h_i denotes the predefined threshold value.

TBM reasoning is performed in two steps. In the first step, basic belief masses m are assigned to the subsets $A_i = \{\forall f_j | \lambda_{i,j} \neq 0\}$ and $B_i = \{\forall f_j \vee ff | \lambda_{i,j} = 0\}$, $i = 1, 2, \dots, K$, $j = 1, 2, \dots, M$, where A_i and B_i are mutually complementary ($m(B_i) = 1 - m(A_i)$).

The belief masses can be set-up as follows

$$m_i(A_i) = \frac{1}{1 + \frac{1-a}{a} \left(\frac{h_i}{r_i}\right)^{2\gamma}}, \quad (7)$$

where a is the belief mass assigned at threshold h_i and γ is an adjustable smoothing parameter.

In the second step, the belief masses $0 \leq m(f_i) \leq 1$ for individual faults and the fault-free case are calculated by using the unnormalized Dempster rule of combination. In the diagnostic context, where features are used as the source of evidence, the rule takes the following form:

$$\begin{aligned} m(f_i) &= (m_1 \oplus m_2 \oplus \dots \oplus m_K)(f_i) \\ &= \prod_{\substack{j=1 \\ f_i \in A_j}}^k m_j(A_j) \prod_{\substack{j=1 \\ f_i \in B_j}}^k m_j(B_j) \end{aligned} \quad (8)$$

As a result, a ranked list of faults is obtained. Portion of belief not assigned to any of the faulty states is assigned to the empty set:

$$m(\phi) = 1 - \sum_{i=1}^{M+1} m(f_i) \quad (9)$$

This measure is referred to as the *strength of conflict*, which may be caused by various sources such as modelling errors, noise and unknown or unforeseen faults. It can be treated as a measure of confidence in the diagnostic results, which provides an interesting feature of this theory.

7 EXPERIMENTAL RESULTS

7.1 Incidence matrix

From the analysis conducted in Section 5 we derived the incidence matrix Λ , shown in Table 2. The faults are labeled as follows:

Fault 1. Rotor unbalance,

Fault 2. Bearing outer race fault,

Fault 3. Bearing inner race fault and

Fault 4. Lack of lubrication.

Besides the listed faults, there is an additional state, the fault-free motor. Since the state does not indicate fault in the remaining part of the paper it will be marked as ff which stands for *fault-free*. Entry “1” in the incidence matrix indicates that the fault affects the corresponding feature, where entry “0” indicated independence between the fault and the corresponding feature.

For feature values we selected the amplitudes of a specific spectral components from the envelope spectrum obtained with the spectral kurtosis method. The corresponding thresholds were determined heuristically, by taking into consideration the quality limits defined by the manufacturer.

Table 2: Incidence matrix Λ

No.	Feature	F1	F2	F3	F4
1	RMS	1	1	1	1
2	f_{rot}	1	0	0	1
3	FTF	0	1	0	1
4	BPFO	0	1	0	1
5	2×BPFO	0	1	0	1
6	BPFI	0	0	1	0
7	2×BPFI	0	0	1	0

7.2 Validation of the diagnostic system

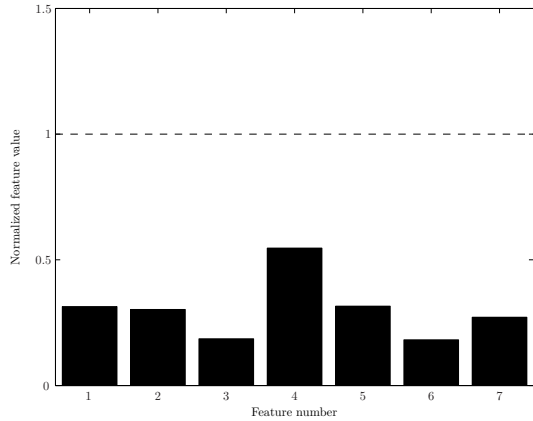
In order to evaluate the performance of the diagnostic system three different fault cases are presented: fault-free, rotor unbalance fault and bearing outer race fault. Feature values have been normalized, by dividing the feature value with the corresponding threshold, thus in all following figures the threshold, marked with dashed line, has value of “1”.

In case of fault-free motor (Figure 7), all features are below the threshold. The algorithm assigns almost all belief to fault-free case (marked as ff). The *strength of conflict* is almost zero, $m(\phi) = 0.096$. High belief mass assigned to the fault free case and low strength of conflict undoubtedly confirms the fault-free case. This is expected since all the features have significantly lower values than the corresponding thresholds.

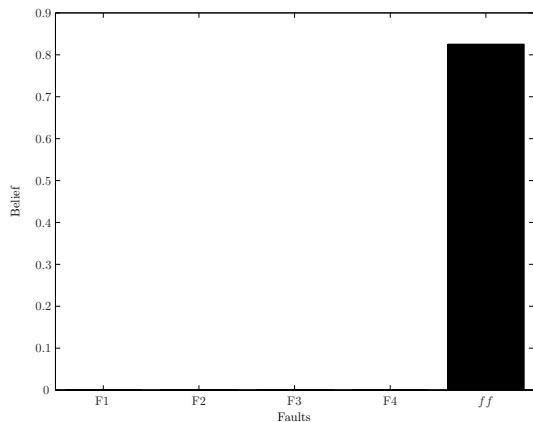
Contrary to the first case, some features in the case of unbalanced rotor (Fault 1) have much higher values than the corresponding thresholds. The diagnosis algorithm properly classifies this case with a belief $m(f_1) = 0.7$ and *strength of conflict* $m(\phi) = 0.285$ (Figure 8).

The last case represents a motor which has a bearing that was not properly mounted. The algorithm assigns a belief $m(f_2) = 0.28$ to the bearing outer race fault and $m(f_1) = 0.15$ to the fault-free case (Figure 9). Additionally the *strength of conflict* is $m(\phi) = 0.57$. The algorithm’s decision for this case is ambiguous. However, the high strength of conflict indicates high uncertainty in the decision, and in such cases additional examination should take place. Although for this case the algorithm failed to provide distinctive decision on a particular fault, it assigned low belief that the examined motor was fault-free.

The benefit of using the transfer belief model is most clearly visible in the last case. The boolean

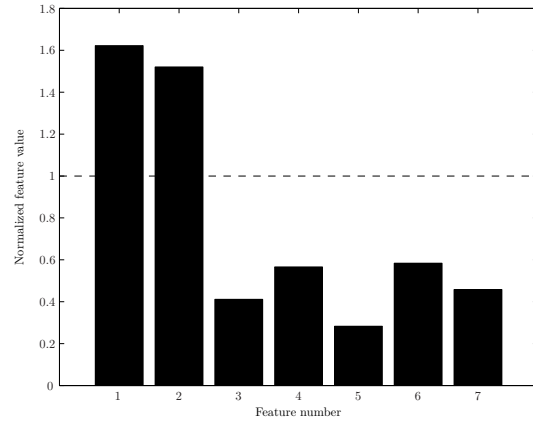


(a) Normalized feature values (feature value divided by corresponding thresholds)

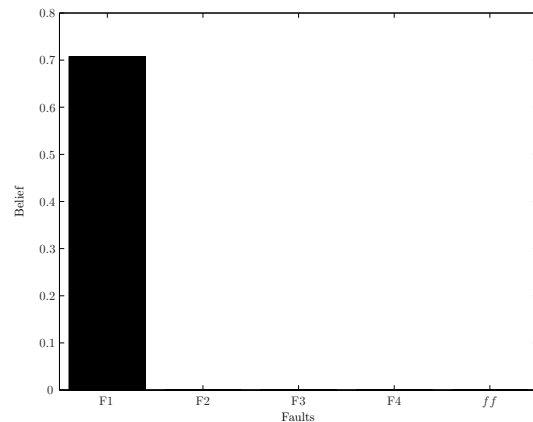


(b) Belief masses for each fault

Figure 7: Fault-free case



(a) Normalized feature values (feature value divided by corresponding thresholds)



(b) Belief masses for each fault

Figure 8: Rotor unbalance

logic would have decided that the motor was fault-free since all features have values lower than corresponding thresholds. On the other hand, the TBM assigned bigger belief mass to the particular fault but most importantly it assigns lower belief mass to the fault-free case and high strength of conflict. Furthermore TBM has the ability to react properly on unforeseen faults. In such cases, the method will not assign belief mass to any existing fault, or the values will be near 0, but the strength of conflict parameter would get large values approaching 1.

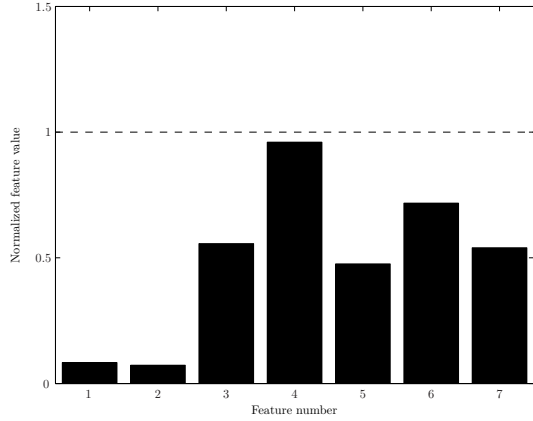
8 CONCLUSION

The aim of this paper was to evaluate the effectiveness of end quality assurance system. Due to the strict production quality standards the fault detection procedure had to be able to detect even the smallest deviations from the fault-free motor. The use of spectral kurtosis for the feature extraction process has enabled a significant increase in sensitivity. The method allows a systematic approach in finding the frequency band where the impulses generated by localized faults are most clearly visible. Features extracted from such a selected band are good indicators of a presence of a particular fault.

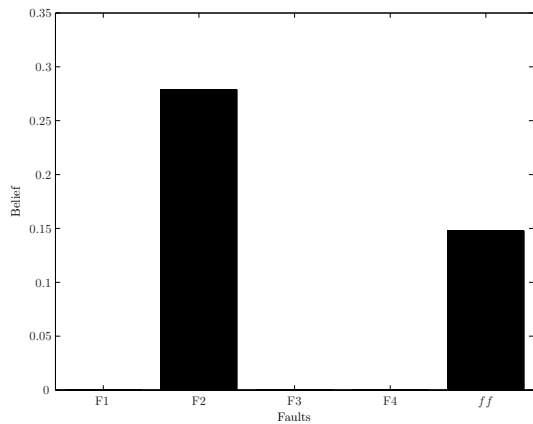
Based on these features a diagnostic procedure is performed employing transferable belief model. Unlike the most machine learning approaches, TBM method does not require experimental runs for training, since the knowledge is incorporated within the incidence matrix. Furthermore the result of this method is a ranked list of possible faults with an appropriate belief assigned to each one. Another asset of the TBM method is the strength of conflict parameter. This parameter provides extra information about the uncertainty of the diagnostic process, which is a valuable information in the decision process, which becomes quite apparent in the cases of unforeseen faults. We can conclude that the approximate reasoning approaches, like the TBM, in conjunction with an effective feature extraction method, like the spectral kurtosis, represent an effective diagnostic tool.

ACKNOWLEDGMENTS

The authors would like to thank Nader Sawalhi from the School of Mechanical and Manufacturing Engineering, The University of New South Wales, for providing the scripts for Spectral Kurtosis.



(a) Normalized feature value (feature value divided by corresponding thresholds)



(b) Belief masses for each fault

Figure 9: Bearing outer race fault

NOMENCLATURE

<i>BPFO</i>	Ball pass frequency outer (race)
<i>BPFI</i>	Ball pass frequency inner (race)
<i>FTF</i>	Fundamental train frequency
<i>BSF</i>	Ball spin frequency
<i>Z</i>	Number of bearing roller elements
<i>D</i>	Bearing pitch diameter
<i>d</i>	Bearing ball diameter
α	Bearing contact angle
f_{rot}	Bearing inner race rotational frequency
$x(t)$	Faulty bearing vibrations
$y(t)$	Faulty bearing measured vibrations
$n(t)$	Noise
$s(t)$	System's impulse response
τ_i	Random time lag between two consecutive pulses

REFERENCES

(Antoni and Randall, 2006) J. Antoni and R.B. Randall. The spectral kurtosis: a useful tool for characterising non-stationary signals. *Mechanical Systems and Signal Processing*, 20:282–307, 2006.

(Antoni, 2006) J. Antoni. The spectral kurtosis: application to the vibratory surveillance and diagnostics of rotating machines. *Mechanical Systems and Signal Processing*, 20:308–331, 2006.

(Antoni, 2007) J. Antoni. Cyclic spectral analysis of rolling-element bearing signals: Facts and fictions. *Journal of Sound and Vibration*, 304:497 – 529, 2007.

(Benko *et al.*, 2005) U. Benko, J. Petrovčić, D. Juričić, J. Tavčar, and J. Rejec. An approach to fault diagnosis of a vacuum cleaner motors based on sound analysis. *Mechanical Systems and Signal Processing*, 19:427 – 445, 2005.

(Didier *et al.*, 2007) G. Didier, E. Ternisien, O. Caspary, and H. Razik. A new approach to detect broken rotor bars in induction machines by current spectrum analysis. *Mechanical Systems and Signal Processing*, 21:1127–1142, 2007.

(Dwyer, 1983) R. Dwyer. Detection of non-gaussian signals by frequency domain kurtosis estimation. *Acoustics, Speech, and Signal Processing, IEEE International Conference on ICASSP*, 8:607–610, 1983.

(Ho and Randall, 2000) D. Ho and R. B. Randall. Optimisation of bearing diagnostic techniques using simulated and actual bearing fault signals. *Mechanical Systems and Signal Processing*, 14:763–788, 2000.

(Isermann and Ballé, 1997) R. Isermann and P. Ballé. Trends in the application of mode-based fault detection and diagnosis of technical processes. *Control Engineering Practice*, 5:709–719, 1997.

(Isermann, 2000) R. Isermann. *Issues of fault diagnosis for dynamic systems*, chapter Integration of Fault Detection and Diagnosis Methods, pages 15–50. Springer, 2000.

(Jack and Nandi, 2001) L. B. Jack and A. K. Nandi. Fault detection using support vector machines and artificial neural networks augmented by genetic algorithms. *Mechanical Systems and Signal Processing*, 16:373–390, 2001.

(Jardine *et al.*, 2006) A.K.S. Jardine, D. Lin, and D. Banjević. A review on machinery diagnostics and prognostics implementing condition-based maintenance. *Mechanical Systems and Signal Processing*, 20:1483–1510, 2006.

(Juričić *et al.*, 2001) D. Juričić, O. Moseler, and A. Rakar. Model-based condition monitoring of an actuator system driven by a brushless dc motor. *Control Engineering Practice*, 9:545–554, 2001.

(Kar and Mohanty, 2006) C. Kar and A. R. Mohanty. Monitoring gear vibrations through motor current signature analysis and wavelet transform. *Mechanical Systems and Signal Processing*, 20:158–187, 2006.

(Leia *et al.*, 2008) Yaguo Leia, Zhengjia Hea, Yanyang Zia, and Xuefeng Chena. New clustering algorithm-based fault diagnosis using compensation distance evaluation technique. *Mechanical Systems and Signal Processing*, 22:419–435, 2008.

- (McFadden and Smith, 1984) P.D. McFadden and J.D. Smith. Vibration monitoring of rolling element bearings by the high-frequency resonance technique - a review. *Tribology International*, 17:3–10, 1984.
- (Rakar and Juričić, 2002) A. Rakar and Đ. Juričić. Diagnostic reasoning under conflicting data: the application of the transferable belief model. *Journal of Process Control*, 12:55–67, 2002.
- (Randall *et al.*, 2001) R. B. Randall, J. Antoni, and S. Chobsaard. The relationship between spectral correlation and envelope analysis in the diagnostics of bearing faults and other cyclostationary machine signals. *Mechanical Systems and Signal Processing*, 15:945 – 962, 2001.
- (Röpke and Filbert, 1994) K. Röpke and D. Filbert. Unsupervised classification of universal motors using modern clustering algorithms. In *Proc. SAFE-PROCESS'94, IFAC Symp. on Fault Detection, Supervision and Technical Processes*, II:720–725, 1994.
- (Rubini and Meneghetti, 2001) R. Rubini and U. Meneghetti. Application of the envelope and wavelet transform and analyses for the diagnosis of incipient faults in ball bearings. *Mechanical Systems and Signal Processing*, 15:287–302, 2001.
- (Samanta, 2004) B. Samanta. Gear fault detection using artificial neural networks and support vector machines with genetic algorithms. *Mechanical Systems and Signal Processing*, 18:625–644, 2004.
- (Sasi *et al.*, 2001) B. Sasi, A.. Payne, B. York, A.. Gu, and F. Ball. Condition monitoring of electric motors using instantaneous angular speed. In *paper presented at the Maintenance and Reliability Conference (MARCON), Gatlinburg, TN., 2001.*
- (Sawalhi *et al.*, 2007) N. Sawalhi, R.B. Randall, and H. Endo. The enhancement of fault detection and diagnosis in rolling element bearings using minimum entropy deconvolution combined with spectral kurtosis. *Mechanical Systems and Signal Processing*, 21:2616–2633, 2007.
- (Singh and Kazzaz, 2009) G.K. Singh and S. A. Kazzaz. Isolation and identification of dry bearing faults in induction machine using wavelet transform. *Tribology International*, 42:849–861, 2009.
- (Smets and Kennes, 1994) P. Smets and R. Kennes. The transferable belief model. *Artificial Intelligence*, 66:191–234, 1994.
- (Staszewski, 1998) W. J. Staszewski. Wavelet based compression and feature selection for vibration analysis. *Journal of Sound and Vibration*, 211:735 – 760, 1998.
- (Tandon and Choudhury, 1999) N. Tandon and A. Choudhury. A review of vibration and acoustic measurement methods for the detection of defects in rolling element bearings. *Tribology International*, 32:469–480, 1999.
- (Tinta *et al.*, 2005) D. Tinta, J. Petrovic, U. Benko, Đ. Juričić, A. Rakar, M. Žele, J. Tavčar, J. Rejec, and A. Stefanovska. Fault diagnosis of vacuum cleaner motors. *Control Engineering Practice*, 13:177–187, 2005.
- (Wang, 2001) Wenyi Wang. Early detection of gear tooth cracking using the resonance demodulation technique. *Mechanical Systems and Signal Processing*, 15:887–903, 2001.
- (Xu and Marangoni, 1994a) M. Xu and R.D. Marangoni. Vibration analysis of a motor-flexible coupling-rotor system subject to misalignment and unbalance, part i: Theoretical model and analyses. *Journal of Sound and Vibration*, 176:663–679, 1994.
- (Xu and Marangoni, 1994b) M. Xu and R.D. Marangoni. Vibration analysis of a motor-flexible coupling-rotor system subject to misalignment and unbalance, part ii: Experimental validation. *Journal of Sound and Vibration*, 176:681–691, 1994.
- (Zarei and Poshtan, 2007) J. Zarei and J. Poshtan. Bearing fault detection using wavelet packet transform of induction motor stator current. *Tribology International*, 40:763–769, 2007.